



Encoding and decoding of the information in the honeybee waggle dance

Zhengwei Wang¹ · Xiuxian Chen² · Ryuichi Okada³ · Stefan Walter² · Randolph Menzel² 

Received: 6 January 2025 / Accepted: 7 April 2025
© The Author(s) 2025

Abstract

Communication processes are characterized by three components: the encoding of a message by the sender, the content of the message, and the process of decoding by the receiver. In honeybee waggle dance communication, the dancing bee encodes the vector as defined by the distance and direction of its outbound flight; the content of the message is a vector that defines a location by its endpoint in a rectangular (Cartesian) or circular diagram; and the dance follower (the recruited bee) translates (decodes) this message into search behavior. Analyses of this communication process have so far depended on the experimenter's knowledge of the geographic location of the hive and the feeder. We applied an approach fully independent of the experimenter's knowledge by quantifying the encoding process by video recording the dance behavior (the waggle runs) and tracking the recruits' flights with harmonic radar. The vector code of the dancer and the search pattern of the recruits led to 2D density distributions that are embedded in the landscape. These density maps (heatmaps) of the encoding and decoding processes were compared quantitatively. We found (1) a non-linear relation between the distance code (number of waggles per waggle run) and the centroid of the search, (2) the dependence of the search pattern on the landscape structure, and (3) effects of the training procedure of the dancers. Importantly, recruits search more precisely than expected from the distribution of vector endpoints as encoded in the dancers' waggle runs. The high search precision can be modeled by assuming an averaging over eight waggle runs, but other phenomena may also be involved (systematic deviations in the vector code, structure of the landscape memory). The high precision of the recruits' search pattern explains why previous analyses of the dance communication of bees are largely adequate.

Significance statement

Communication involves encoding, message transmission, and decoding. In honeybee waggle dance communication, the dancer encodes a vector representing a location, which recruits decode into search behavior. Traditional analysis relied on experimenters' geographic knowledge. We used for the first time an approach combining video recordings and harmonic radar tracking to compare the dancers' vector code with the recruits' search patterns and found (1) a nonlinear relationship between distance encoding and search centroid, (2) landscape-dependent search patterns, (3) effects of training on dancers, and (4) importantly, a more precise search pattern produced by the recruits than expected from the distribution of the vector endpoints, likely due to averaging over multiple waggle runs and to landscape memory. This explains the robustness of previous analyses of dance communication.

Keywords *Apis mellifera* · Radar tracking · Dance-followers · Heatmaps of search · Heatmaps of dance messages · Averaging dance message

Communicated by O. Rueppell.

✉ Randolph Menzel
menzel@neurobiologie.fu-berlin.de

¹ CAS Key Laboratory of Tropical Forest Ecology,
Xishuangbanna Tropical Botanical Garden, Chinese
Academy of Sciences, Menglun, Xishuangbanna
666303, China

² Institute for Biology, Neurobiology, Freie Universität Berlin,
14195 Berlin, Germany

³ Department of Biology, Graduate School of Science, Kobe
University, Kobe 657-8501, Japan

Introduction

The honeybee's waggle dance is an intriguing example of multisensory convergence, central processing, learning, memory retrieval, and symbolic information transfer (von Frisch 1923). In this sense, waggle dance communication follows the structure of communication processes in general. They are characterized by three components: the encoding of a message by the sender, the content and transmission of the message, and the process of decoding by the receiver. In honeybee waggle dance communication, the dancing bee encodes the vector as defined by the distance and direction of its outbound flight; the content of the message is a vector that defines a location by its endpoint in a rectangular (Cartesian) or circular diagram; and the dance follower (the recruited bee) translates (decodes) this message into search behavior. So far, the content of the message and its transmission have been derived from the experimenter's geographic knowledge (the location of the hive and the feeder). Here we ask how the encoding and decoding processes are related quantitatively, making the analysis of the message content independent of the experimenter. This unique approach allows us to quantify the message fully from the senders' and receivers' sides. In essence, we test the hypothesis whether the receiver of the dance message steers to the geographic location of the dance indicated place, a knowledge the receiver derives from its landscape memory.

The waggle dance consists of multiple rounds, each of which is divided into a straight waggle run and a curved return run (review: von Frisch 1967). The direction of the waggle run relative to gravity on the vertical comb codes the direction of the outbound flight relative to the sun azimuth at the time of day in question. The distance known to the experimenter correlates with the several parameters of each waggle round, for example the duration of the full round including the waggle run and the return run, the duration of the waggle run, and the number of waggles (von Frisch 1967; Fig. 8, p.100, Haldane and Spurway 1954; Preece and Beekman 2014; Schürch et al. 2019; Kohl and Rutschmann 2021). We have previously evaluated the number of waggles per waggle run because this parameter varies less than the other parameters (Menzel and Galizia 2024). Thus, the two parameters, distance and direction, define a vector in a circular diagram, and the endpoints of this vector (more precisely the polar vector) can be converted into a Euclidean space with the hive at the local position with $x=0$ and $y=0$. It is the spatial distribution of the x and y values of the vector endpoints and their distribution that are used here for a quantitative comparison with the decoding process as expressed in the spatial distribution of radar measurements (radar fixes) during the recruits' search flights.

Under the assumption that the recruits extract vector information comparable to what the experimenter has, several highly relevant questions have been addressed in previous studies: for example, do bees average directions in the waggle dance to determine a flight direction (Tanner and Visscher 2008; De Marco et al. 2008), do individual dancers have their own distance functions (Schürch et al. 2016), how accurately can the distance be predicted from the duration of the waggle run (Schürch et al. 2013), does the variance in the direction code depend on the angle to gravity (Couvillon et al. 2012), is the error in waggle dance information a colony-level adaptation or a process intrinsic to the encoding process (Preece and Beekman 2014), how is sequentially experienced dance information integrated over time (Chatterjee et al. 2019; see also the recent review by Kohl and Rutschmann 2021)? Obviously, these highly valuable studies are limited by the fact that the transfer from encoding to decoding is assumed to be a 1:1 process, and the decoding process does not yield additional information that is available to the recruit. We show here that this assumption is close to being correct.

Our own approach was possible because we tracked the flights of the recruits with harmonic radar. The density distribution of the radar fixes (the x and y locations of each radar measurement— each radar fix— during the search) allows us to quantify and calibrate the search behavior in two-dimensional Euclidean space as defined by x and y values (with the hive at $x=0$, $y=0$), and compare it with the 2D distributions of the dance vector endpoints. Applying the information from these 2D-density functions, we address the following questions. How accurate are the distributions of the dance vector endpoints and the search patterns of the recruits? Does the distance code vary with distance, or is it a linear function over distance? Since the flights of recruits consist at first of straight flights (here called vector flights) and then of tortuous search flights, do the endpoints of the vector flights center on the geographic location of the feeder? If not, how are the deviations of the vector flight corrected during search flights? Do the endpoints of the vector flights and the distributions of the search flights depend on the landscape structure?

Methods

Experimental site, honeybee colonies, feeders for the dancers

Four different experimental feeder sites (F1, F2, F3, F6) were established in a structured agricultural landscape dominated by large grass fields with trees and bushes, pathways, creeks and roads. Two hive locations were established, hive

1 at earth coordinates: 50.813910° N, 8.872658° E, hive 2 at earth coordinates: 50.815156° N, 8.913284° E (Fig. 1). The colonies were housed in a two-frame observation hive with approximately 3500 bees. Many of these bees were marked with two-digit number tags as described previously (Menzel 2015). The number tags came in five colors and were positioned on the bee thorax in four different directions relative to the body length axis, allowing us to mark up to 1950 individual bees (excluding numbers that could be confused, such as 66 with 99, or 69 with 96).

The distances and directions of the feeders from the respective hives were as follows. The training sites for hive 1 were: F1: 431 m, 344° (earth coordinates: 50.817761°N, 8.870755° E); F2: 387 m, 65° (earth coordinates: 50.815673°N, 8.877301° E); F3: 773 m, 81° (earth coordinates: 50.815384° N, 8.883226° E). The training site for hive 2 was: F6: 2300 m, 270° (earth coordinates: 50.814054°N, 8.878770° E). The data for training sites F1 and F2 were collected after more than two weeks of training to these sites. A different procedure was applied to training sites F3 and F6: the feeders were moved in steps from the respective hives to their final destination, with feeder sites in-between, and the data were collected just two days

after the final site had been reached. The feeders were used consecutively, and two different colonies were set up at the two hive locations. The reason for locating hive 2 further away from the radar was that the radar range is limited to a radius of 900 m (see below), and the dancers in hive 2 needed to indicate a location within the radar range so that recruits search flights could be tracked. An unavoidable consequence was that no vector flights could be tracked for recruits from hive 2 (see below). Both hives were set up in the area more than two weeks before the experiments started, ensuring that the foragers had explored the area. The marking of the foragers with number tags started after these two weeks and was conducted early in the morning or late in the afternoon to ensure that only experienced foragers were included in the experiment.

Each visit of the foragers acting as dancers was confirmed at the feeder at the level of the individual animal, which was additionally marked with a white dot on the abdomen, allowing immediate identification of whether the respective dance had been performed for a particular experimental feeding site. A complete protocol of all visits to the feeders was established, and a relatively small number of potential dancers were trained. No odors were used at the feeders,

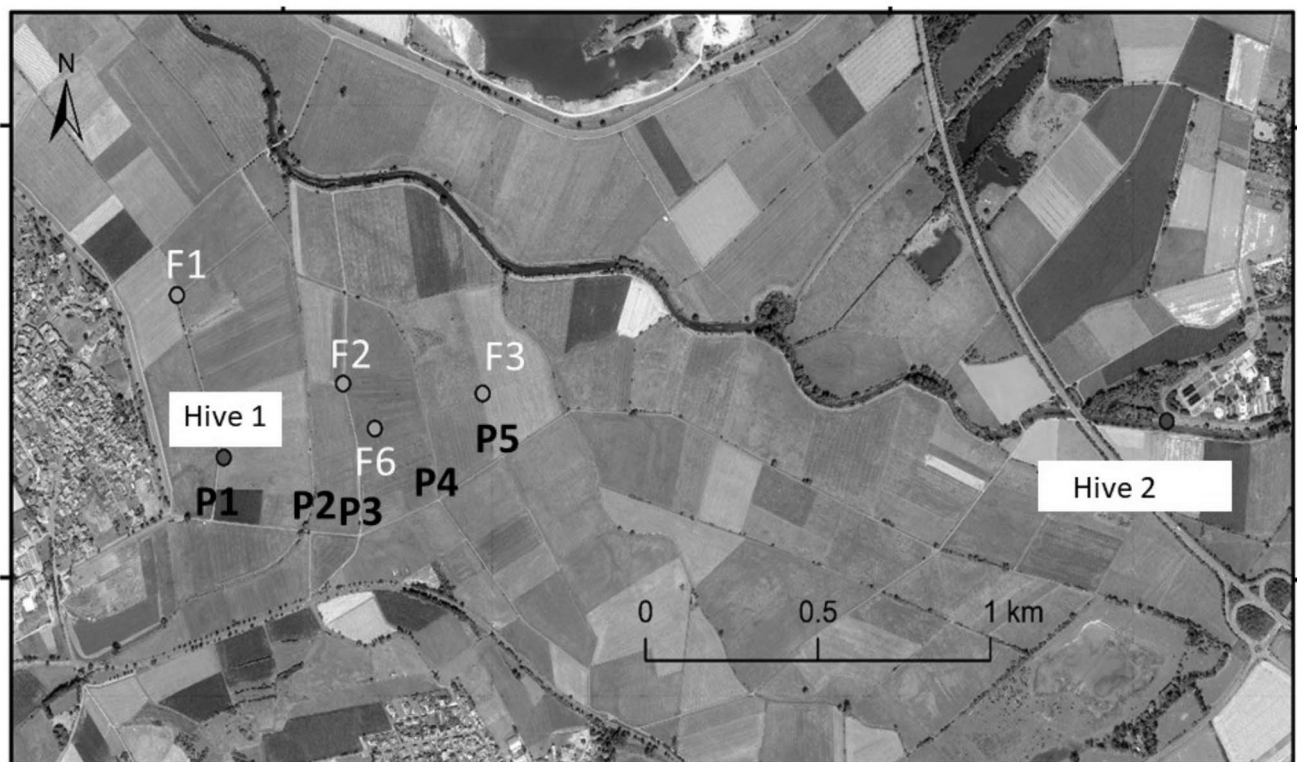


Fig. 1 Landscape with all relevant locations. Hive 1 is located at the site of the radar. Feeders F1, F2, F3 are the training locations for hive 1. Feeder F6 is the location to which dancers from hive 2 were trained. Hive 2 was located 2300 m east of the feeder, and the dancers were trained stepwise from the hive to the location of F6 to ensure that it lay within the range of the radar. P1– P5 mark five paths that run roughly

parallel approximately from south to north (referred to here as salient elongated ground structures). Note that F1 is located on P1, and the dancers flew along P1. F2 and F3 are also located on paths (P3 and P5 respectively), but the dancers flew across frequently mown, even grassland

either during the stepwise training or at its final location. The feeders were plastic jars filled with sucrose solution at different concentrations depending on the need to stimulate dances. They stood on a small table without any color mark. Recruits were removed from the colony after recording their flights to ensure that they were tested only once.

Video-recording, analysis of dances and selection of the recruits to be followed by harmonic radar

Waggle dance behavior was recorded by video at 50 Hz. The illumination of the observation hive was diffuse and by dim natural light. No direct natural light reached the dance floor. The ambient light in the cabin housing the observation hive was very low. The videos were analyzed by hand using a frame-to-frame procedure, measuring the number of waggles per run and the direction relative to gravity. A waggle is a body movement from the midline to the right (or the left), then to the left (or the right), and back to the midline. The beginning and end of the waggle run was defined by the first or last blurred single frame. The number of waggles per run was counted, and the walking trajectory was tracked on a transparent sheet with a marker, allowing the direction relative to the vertical to be determined, as indicated by a plumb

line. The directions were converted to the corresponding directions relative to the sun azimuth at the particular time of the waggle dance by using the Python tool, Astropy (<http://www.astropy.org/acknowledging.html>). The accuracy of timing was set to 5 min.

It was not possible to video-record the dances during the identification and selection of the recruits whose flight was tracked by radar. In this situation the recruits were identified visually by their individual numbers. When one of the recruits left the dancer after following it for several rounds and then steered towards the exit, its number was announced to a co-experimenter in front of the hive. This bee was then captured, stored in a veil in the dark for a few minutes, equipped with a radar transponder, and released close to the hive exit. Each recruit was used for a test only once and removed from the colony because all the released recruits arrived back at the hive.

Figure 2 shows two examples of fully tracked recruits with their initial vector flight, the search flight and the straight homing flight. Homing flights are not further considered here because all the bees returned home on fast and straight flights. Homing flights start after the last turn during search and end at the hive. The transitions from the vector flight to the search flight and from the search flight to the

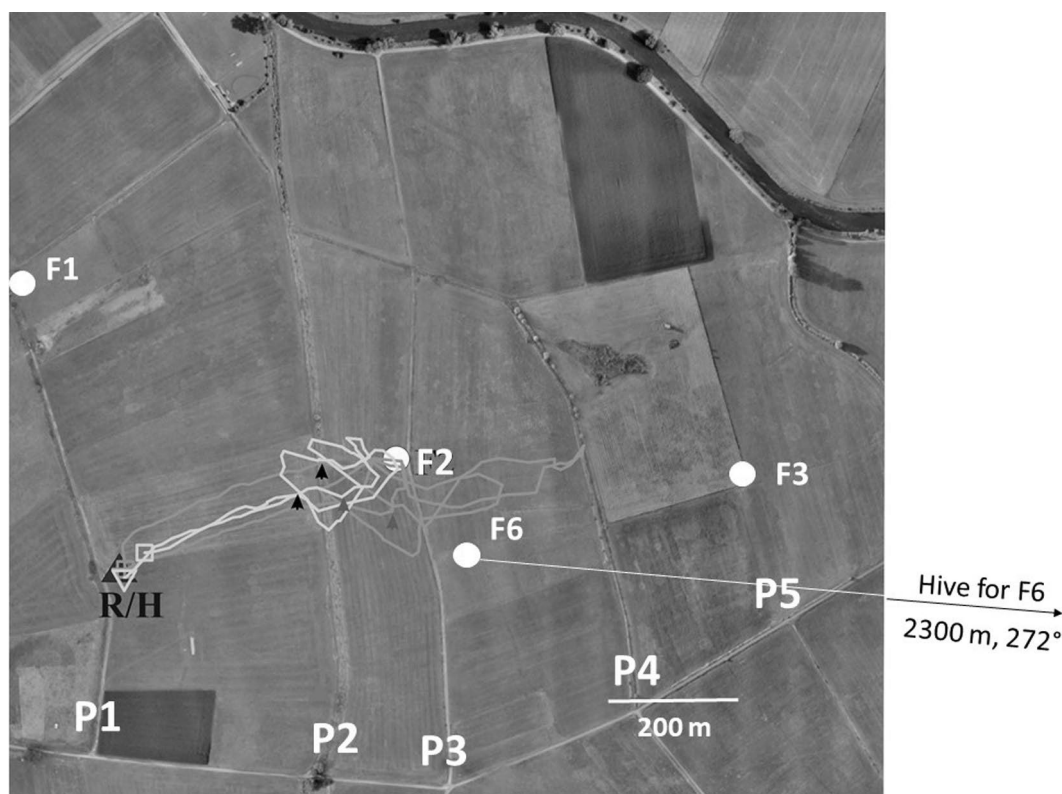


Fig. 2 Two representative flight trajectories of recruits for F2 (yellow and orange tracks). The squares mark the start of the fast and straight vector flight, and the triangle the end of the vector flight. The upward-pointing black arrows mark the transition from the vector flight to the

tortuous search flight, and the upward-pointing red arrows the transition from the end of the search flight to the fast and straight homing flight. Thus, the part between the respective arrows marks the search flight

homing flight were characterized by a sharp turn of $\geq 60^\circ$, with straight stretches before and after the turn comprising at least three fixes each. Sometimes, the transition between these three segments of the flight trajectory was less obvious, as when the vector flight or homing flight followed a gradual change of flight direction. In these (few) cases, the overall direction was taken into consideration. The search flight was taken to be the part between the end of the vector flight and the beginning of the homing flight.

Tracking bees with a harmonic radar was undertaken as previously described (Cheeseman et al. 2012; Riley et al. 2003). We used a system with a sending unit consisting of a 9.4 GHz radar transceiver (Raytheon Marine GmbH, Kiel, NSC 2525/7 XU) combined with a parabolic antenna providing approximately 44 dBi. The transponder fixed to the thorax of the bee consisted of a dipole antenna with a low-barrier Schottky diode HSCH-5340 of centered inductivity. The second harmonic component of the signal (18.8 GHz) was the target for the radar. The receiving unit consisted of an 18.8 GHz parabolic antenna, with a low-noise pre-amplifier directly coupled to a mixer (18.8 GHz oscillator) and a downstream amplifier with a 90 MHz ZF-filter. A 60 MHz ZF-signal was used for signal recognition, leading to a fixing of the bee carrying the transponder. The transponder weighed 10.5 mg and was 11 mm long. We used a silver or gold wire with a diameter of 0.33 mm and a loop inductance of 1.3 nH. The range of the harmonic radar was set to 0.5 nautical miles in most experiments (to 0.75 nm in some tests after training to F3 and F6). The frequency of radar fixes was every 3 s. The raw radar output was captured from the screen at a frequency of 1 Hz, stored as bitmap files, and further analyzed offline by a custom-made program that detected and tracked radar signals (fixes) and converted circular coordinates into Cartesian coordinates,

taking into account multiple calibration posts in the environment. Finally, the fixes were displayed in a calibrated geographic map created with the software Pix4D from aerial images (Strecha et al. 2012) taken with a commercial drone (DYI Inspire). If no fixes were received from a bee for more than 30 s, the flight trajectory was interrupted, and the last, as well as the first, fix before and after the interruption was marked.

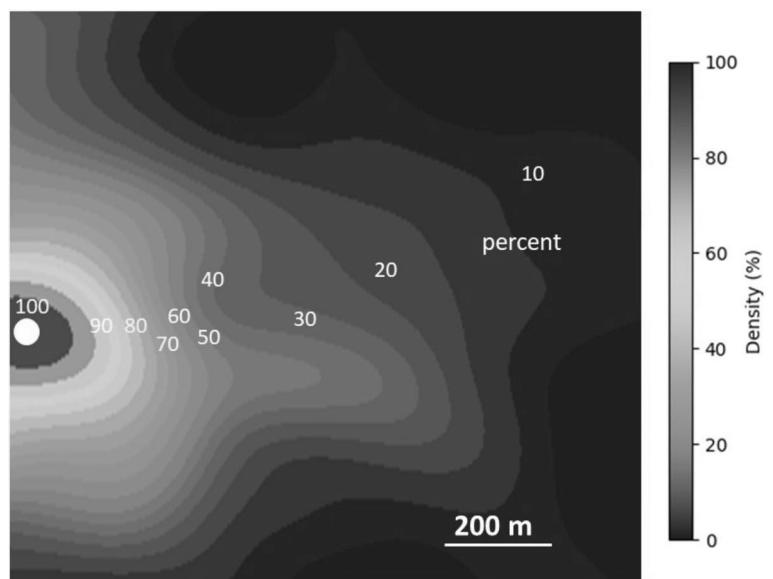
Two-dimensional density maps of radar fixes or dance vector endpoints (heatmaps)

Heatmaps were plotted using a custom script written in Python, taking advantage of its powerful libraries for data analysis and visualization (pandas, matplotlib, and seaborn; <https://pandas.pydata.org/>, <https://matplotlib.org/>, <https://seaborn.pydata.org/>). The D2 kernels were kept constant across all calculations. Figure 3 shows a section of a heatmap with the color bar coding the steps of normalized density in false color.

Statistics

Quantification of heatmaps and comparison between heatmaps of dance-indicated vector endpoints and the radar fixes of the recruits' flights were undertaken as follows. Since the heatmaps for dance vector endpoints and for recruit search fixes are close to circular, the two distributions were compared by determining the quantity of data in concentric rings around the respective centroid. The area in each ring was the same and was equal to the area around a centroid with a radius of 120 m (Fig. S5). These data were used to determine trends in the proportions along the rings, first applying multivariate Cox PH models separately for the dance and

Fig. 3 Section of the two-dimensional distribution of the density of radar fixes or dance vector endpoints (heatmaps). The x, y coordinates are related to the location of the radar ($x=0$, $y=0$). Hive 1 for feeders F1, F2, and F3 was close to the radar (3 m). Hive 2 for feeder F6 was further away from the radar (2300 m to the east, Fig. 1). The color bar gives the false colors for 5% steps in density grading. The numbers in the figure mark the density grading for every 10% step. The centroid of the heatmap within the area of highest density of fixes was determined by eye (marked with a white dot)



the recruit data. A survival analysis combined with a Cox regression (Su et al. 2022) was applied to the decreasing trends in the number of dance vector endpoints and search fixes that fell in each concentric ring.

A Spearman-rho ranked-order correlation was applied to examine the correlation between the correction angle (Fig. S2: α), defined by the first turn at the transition from vector flights to search flights, and the deviation from the ideal direction to the feeder indicated by the dance (Fig. S2: $\Delta\alpha$).

For the simulation of the averaging effect, each waggle run was converted into x/y coordinates (the coordinate of the hive was [0,0]) based on a distance obtained by using the number of waggles and the optimal scaling factor, and the polar coordinates (angle relative to north). The necessary number of waggle runs was selected randomly using MATLAB, and the x/y coordinates were averaged. Then the averaged x/y coordinates were converted into distance and polar coordinates for direction. This procedure was repeated 10,000 times for each simulation condition. Because one simulation leads to 10,000 distances and directions, the data were sorted by ascending value to obtain an interquartile range (IQR). The IQR is defined as the difference between the lower quartile (25%) and the higher quartile (75%). Hence, if data distributions are wider, the IQR is larger. The IQR was obtained for each condition in which the encoded information from 1, 2, 3, 4, 5, 6, 7, 8, 9, 10, 15, 20, 25, and 50 runs was averaged for each feeder (F1, F2, F3, and F6).

All data leading to the figures are given in the supplementary material (S all tables together).

Results

Encoding

Each waggle run encodes a vector whose endpoint indicates a location if one applies the sun-compass-corrected direction to gravity and a factor that converts the distance measure (traditionally duration of the waggle run, here the number of waggles per waggle run) into the real distance from the hive. The number of waggles per waggle run has already been used as a code for distance by Haldane and Spurway (1954) (see also Couvillon et al. 2012), who inferred from the data, as also reported in von Frisch (1967, p. 100), a constant factor of 70 m per waggle (here called the scaling factor of the distance code) over varying distances. As pointed out above, we are in the unique position that the searches of the recruits collectively yield a center of search that informs us about where in space they expect the feeder indicated by the dancer to be with highest probability. Thus, it is not the knowledge of the experimenter but information from the recruits that allows us to determine the scaling factor and

to examine whether it is constant over different distances and whether it depends on additional parameters (e.g. the history of dance communication, landscape properties). Most importantly, the combined expression of both dance codes (distance and direction) in the form of 2D density distributions (heatmaps and their quantification) allows us to address the question whether the accuracy of the recruits' search differs from what can be expected from the process of encoding by the dancers and the decoding leading to the recruits' search.

The dance data were used to examine the effect of different scaling factors (55 m, 60 m, 70–80 m per waggle) on the density distribution of danced vector endpoints (Fig. S1, S all tables together). As expected, the 2D distribution becomes wider with a rising scaling factor and increasing distance from the real feeder location. From a visual inspection of Fig. S1 we deduce optimal scaling factors of 60 m (for F1 and F2), 70 m (for F3) and 80 m (for F6) indicating a none linear relation between the number of waggles and the distance (Fig. 4). However, this finding is compromised by the fact that we have only 4 data points (centroids of search patterns at different distances). This conclusion is supported by the search pattern of the recruits (see below). The rather close to circular distributions of dance vector endpoints (less closely fitting for F3, see below) allows an additional measure of the indicated location, the angular width of the distribution that contains 50% of the data (angle of 50% capture). The values for the four feeders are as follows: F1: 130°, F2: 132°, F3: 122°, F6: 104°. This indicates increasing precision in the direction code with distance.

Decoding: search behavior of recruits

First, we analyzed the endpoints of the vector flights (Fig. 5). Vector flights terminate well before the indicated feeder location. F1 is located on a gravel road (path 1, Fig. 1) 431 m NNE of hive 1. F2 and F3 were reached by the dancers after flying over rather even grassland. Recruits for F1 performed very short vector flights, and their density distribution is elongated along path 1 (P1 in Fig. 1). Vector flights for F2 terminated approximately two thirds of the distance to F2; for F3 less than halfway to the feeder. The density distribution of the vector endpoints for the F2 recruits is rather circular (as are the distributions of the dance vector endpoints, see above). Interestingly, the heatmap for the F3 recruits is extended between the two paths P3 and P4 (Fig. 1), and F3 is located on path P5. The vector flights of the F6 recruits terminate in two density peaks, one about 400 m less than the full distance to the feeder and one at about the correct distance but shifted southward.

For the F2 recruits, we addressed the question whether they somehow notice the deviation from the ideal direction

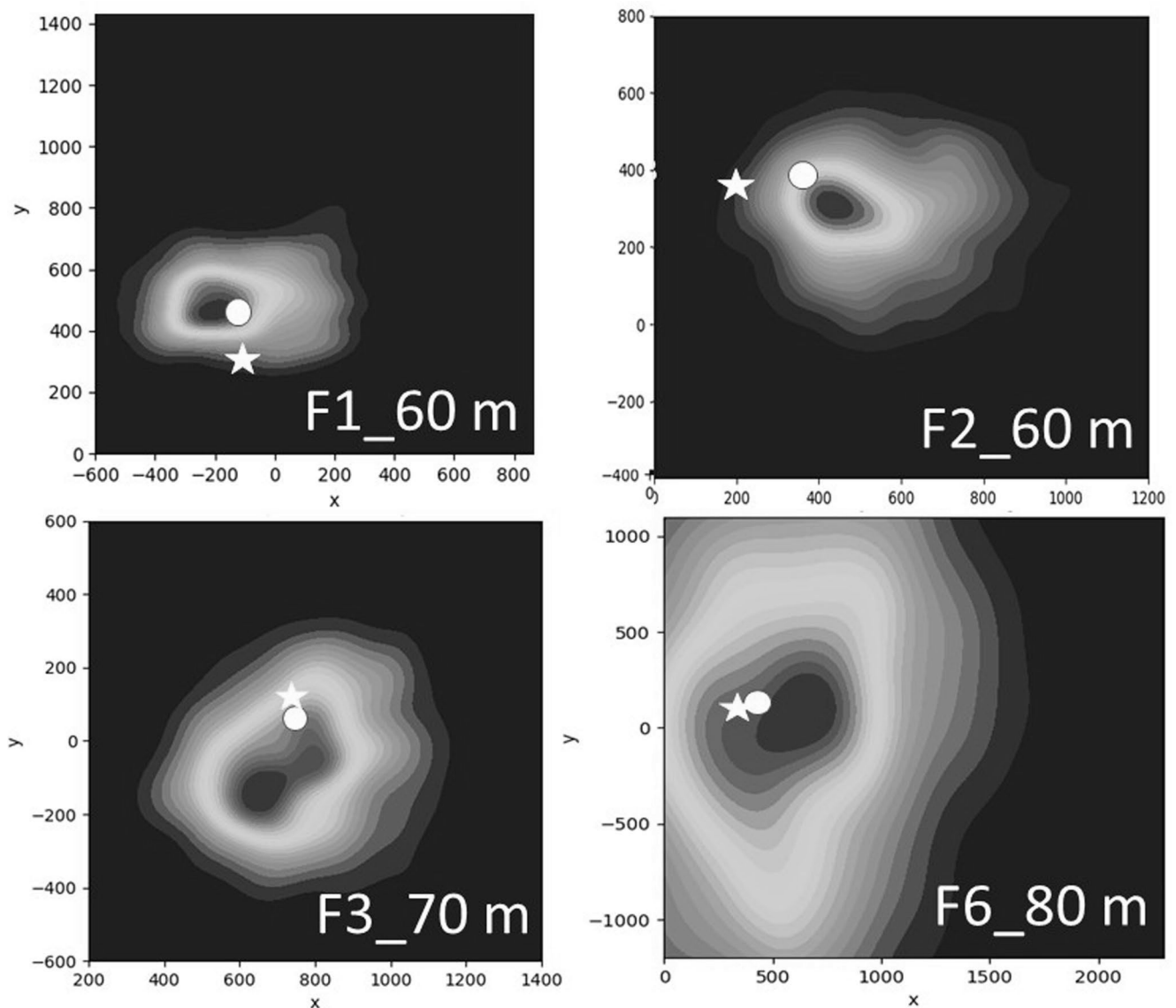


Fig. 4 Heatmaps of waggle dance vector endpoints, the real geographic location of the feeder (white dot), and the centroid of the recruits' search distribution (white star, see Fig. 7). The distribution of the

dance vector endpoint is given for the calibrated scaling factor (CSF), the optimal scaling factor (F1: 60 m, F2: 60 m, F3: 70 m, F6: 80 m). Note the different scales (for data to Fig. 4 see S all tables together)

and correct these errors in their first turn after terminating the vector flight and initiating the search flight. This was done by applying a Spearman-rho ranked-order correlation analysis between the deviation of the vector flight angle ($\Delta\alpha$) from the ideal angle and the first turn (the correction angle, ca.) at the transition to the search flight. Fig.S2 shows a high correlation (correlation coefficient: 0.61), indicating a memory for the ideal direction.

Next, we analyzed the search patterns of the recruits. Figure 6 shows the respective density distributions of the radar fixes together with the locations of the respective feeders, the hive and the line between hive and feeder. Overall, the distributions of search flight fixes are surprisingly narrow and close to the respective feeder. As mentioned in

the Methods and above, feeders F1 and F2 were kept stationary for more than a week whereas feeders F3 and F6 were reached during a stepwise training to their respective final location, and the final location was kept stable for just two days. The most accurate and circular search pattern was found for F2, a feeder that was reached by the dancers (and their recruits) after flying over even grassland. The search pattern of the F1 recruits is elongated along P1 (as are their vector endpoints; see Fig. 5) and focuses on an area at a shorter distance from the hive than F1, an effect most prominent in the vector flights. Elongated ground structures (here the gravel road) have been found to guide bees (Menzel et al. 2018). Thus, the recruits might “expect” the dance-indicated feeder somewhere along this elongated ground

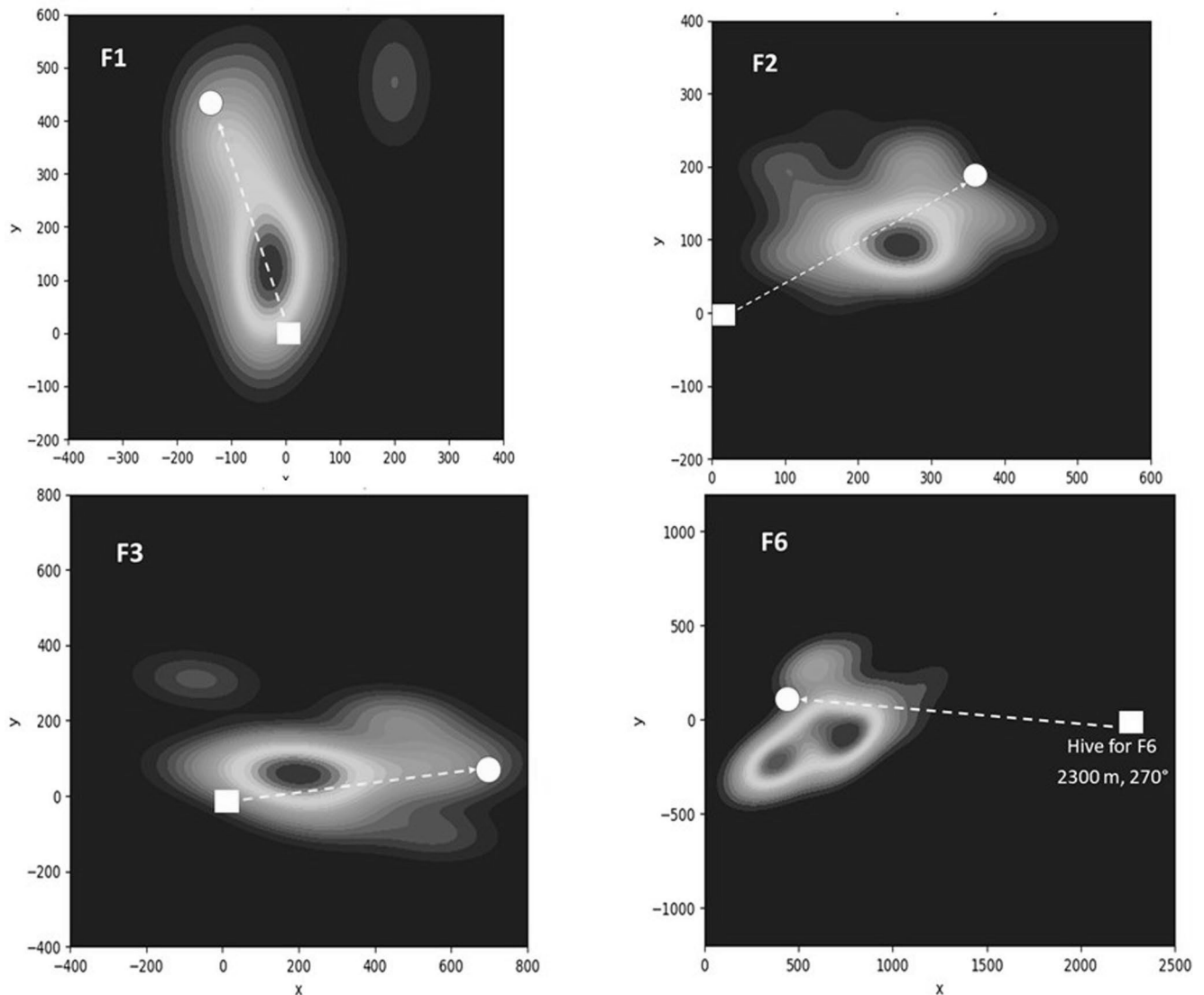


Fig. 5 Density distribution of the endpoints of the vector component of recruits for the four feeder locations F1, F2, F3, F6. The square in the subfigures marks the location of the hive location. The white dot marks

the location of the respective feeder, and the dotted arrow the direct line from the hive to the feeder. The scales differ in the four subfigures for data to Fig. 5 see S all tables together)

structure, possibly starting their tortuous search flights at shorter distances from the hive. Recruits for F3 search at two hot spots, one closer to the location of F3 and one close to the location of the last feeder location before reaching F3 (two days previously). Analyzing the search patterns separately for the individual recruits brings to light that most of the recruits showed this double-peak search pattern, and the few who did not do so searched only around the further destination. We cannot rule out the possibility that a recruit tested for the final location may have followed a dance for a prior location without visiting it, and in such a case the recruit may have remembered the information transmitted by the dance for at least two days.

Of hundreds of recruits tested during our experiments, only three landed on the feeder (F2). One may argue,

therefore, that the search strategy might change to broader search during an ongoing process of searching to a broader search. We plotted heatmaps for the first, the second, third and fourth tenths of fixes for F2 and found the narrowest distribution during the second tenth of fixes (corresponding to the second half of the first minute of search) (Fig. S3). After 1.5 min (third and fourth tenths of fixes), the recruits extended their search pattern, and a few of them flew away from F2, possibly towards natural food sources along the creek in a northeasterly direction far out of the range of the radar (Fig. 1). These patterns indicate a change in the strategy for searching for the feeder, with first an increase and then a decrease in precision in relation to the location of the dance-indicated feeder.

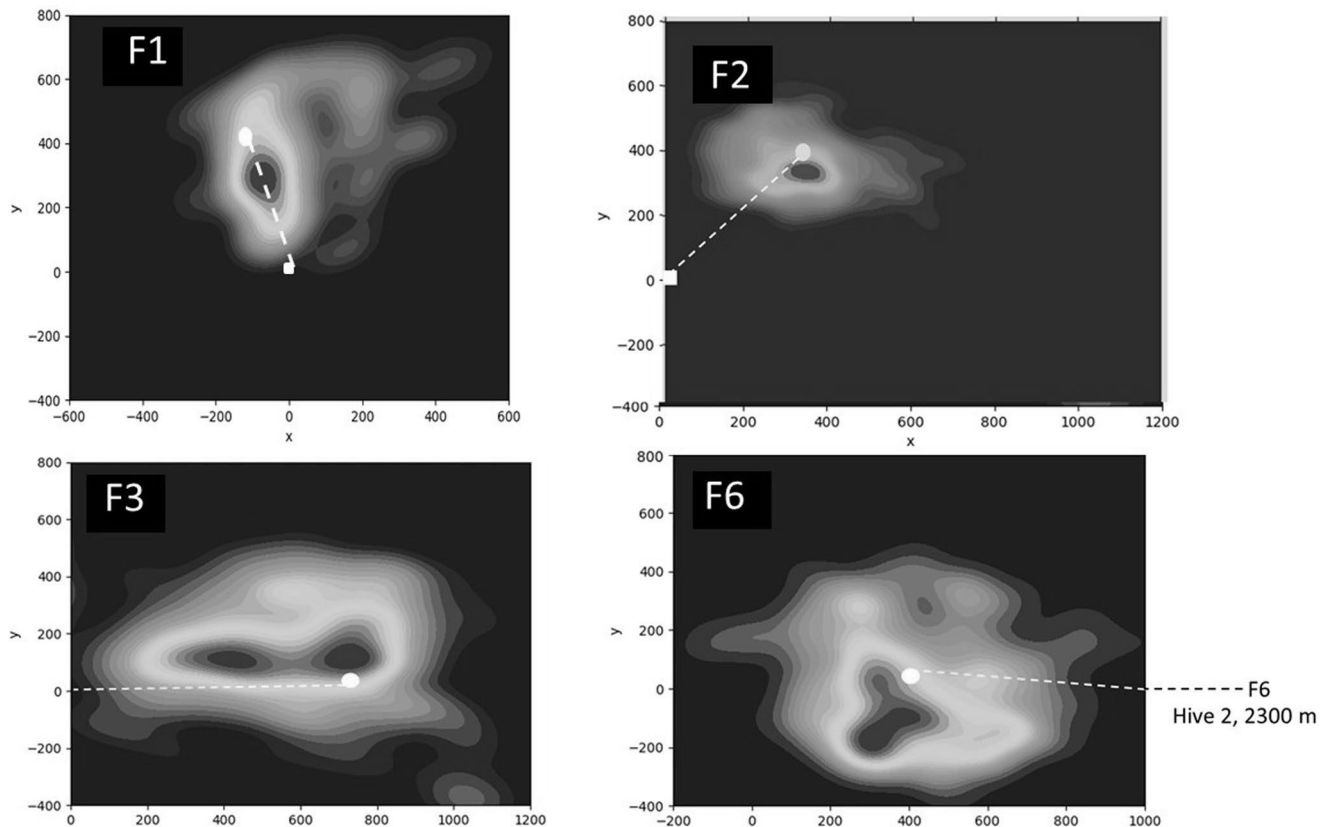


Fig. 6 Density distribution of recruits' search fixes for the four feeders as visualized by heatmaps. The white dot indicates the location of the respective feeder, and the white square the hive (F6 hive 2, 2300 m to

east). The dotted white line gives the direct connection between the hive and the feeder. Note the same scale in all subfigures (for data to Fig. 6 see S all tables together)

Comparison between encoding and decoding

In preparing a comparison between the encoding and decoding processes, we selected the best-fitting 2D distributions of dance vector endpoints for the four feeding sites (Fig. 4). These optimal scaling factors (CSF) lead to the shortest distance between the centroids of the search fixes and the centroids of the 2D distributions of the dance vector endpoints. Figure 7 shows that for F2 the density distribution of dance vector endpoints is much wider than the distribution of search fixes. The area covered by the respective 2D distributions shrinks by a factor of 2.8 (area defined by 50% data points for the dance vector endpoints: 16,280 m², for the recruits' search fixes: 5,810 m²). Similar results were found for the other feeders (compare Fig. 4 with Fig. 6, and Fig. S4). The improvement with distance during the decoding process can be captured by comparing the angle under which the circumference of the 50% capture area is seen from the hive: F2 (distance: 387 m): dance vector endpoints: 132°, recruits' search fixes: 70°, F6: (distance: 2600 m): dance vector endpoints: 104°, search fixes of recruits: 60°. As pointed out above (Fig. 4), CSF differs between the shorter distance of F2 (CSF: 60 m) and the longer distance

of F6 (CSF: 80 m). These results emphasize the importance of relating the encoding and decoding process to the 2D area derived from the joint effect of encoded parameters (distance, direction) rather than isolated parameters. Additional parameters are uncovered by this strategy of analysis (the path-following behavior seen for the recruits for F1, and the sequential training effect as seen for F3: see also below).

The two procedures followed in undertaking a quantitative comparison between the heat maps of the encoding and decoding process are described in Methods, Statistics. Significant differences were found for F1, F2 and F6 but not for F3 between the trends in the dance endpoints and the recruits' search fixes that fall within each concentric ring around the respective centroid (Cox PH model for multivariable analysis: F1, $Z_{446}=2.523$, $p=0.011$; F2, $Z_{661}=8.884$, $p<0.001$; F3, $Z_{552}=0.33$, $p=0.0.742$; and F6, $Z_{446}=2.523$, $p<0.001$: see Fig. S5, data S all tables together). It is unsurprising that the two distributions for F3 are not significantly different because of the double peaks in the recruits' search distribution. As mentioned above, this double peak results from the sequential steps in the training of the F3 dancers (Fig. 4).

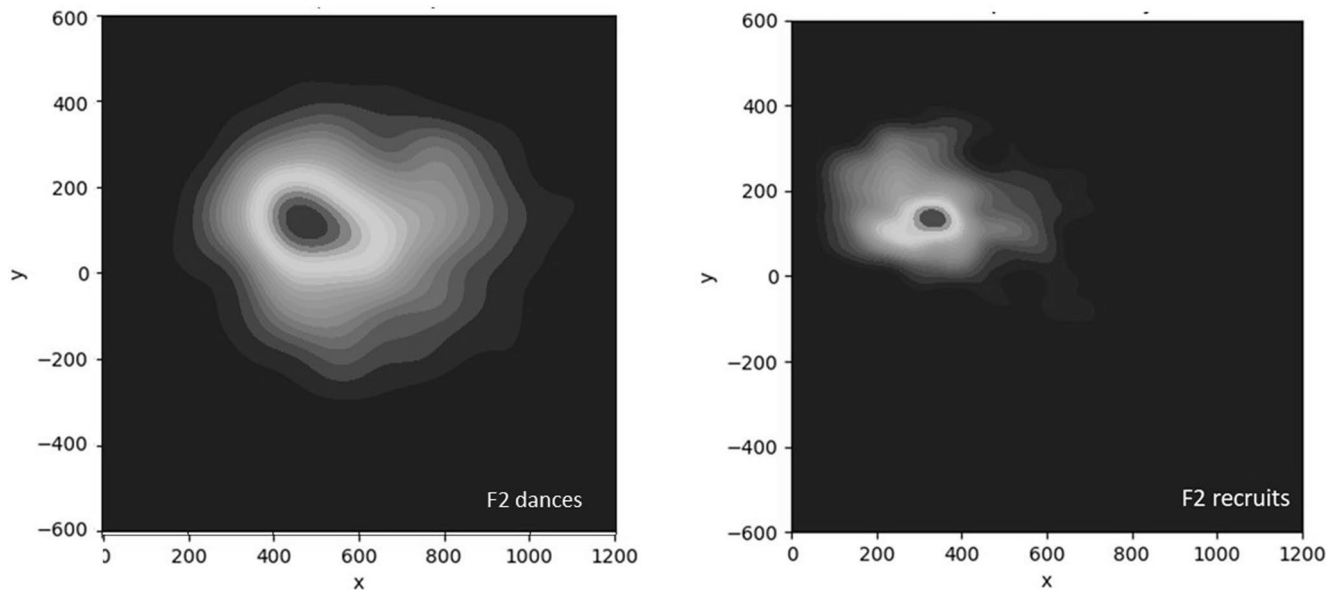


Fig. 7 Comparison of the density distributions of the dance vector endpoints for feeder F2 and the radar fixes of the recruits' search for feeder F2. Note that the heatmaps are plotted on the same scale. Comparisons of the density distributions of the dance vector endpoints (calcu-

lated with the respective optimal scaling factor CSF) and the respective search pattern of recruits for the other three feeding sites can be extracted from Fig. See S7 (for data to Fig. 2 see S all tables together)

Dance-following and the effect of the averaging of waggle runs of one dance

Higher precision in the recruits' search may result from averaging across several dance rounds. Dancers vary in the number of waggle runs performed in one dance, ranging up to more than 100 runs per dance (Seeley et al. 2000). To estimate the effect of averaging, we calculated the heatmaps of dance vector endpoint distributions for different numbers of averaged runs (Fig. 8A for F2 recruits, Fig. S6 for recruits to other feeders). The averaging effect is most drastic during the first six averaged rounds and saturates after more than eight averaged rounds. No dependence on distance was found.

Next, we simulated the averaging effect separately for the distance and the direction code (Fig. 8B, see Statistics). Each step of simulation leads to 10,000 distances and directions. Figure 8B shows the results for distance and direction and for the four feeding sites separately. Most of the gain from averaging is reached by 8 averaged runs. Interestingly, the rank order is different for distance and direction: for distance: F1, F3=F2, F6, for direction: F3, F2, F6, F1. There is a greater effect on the distance code.

Discussion

The decoding process has previously been approached by attempts to prove von Frisch's conclusion correct (Riley et al. 2005) and characterize navigation (review: Menzel 2023). Here we present for the first time a combined analysis of the encoding and decoding processes of waggle dance communication. Several topics can thereby be addressed that have been discussed with data only on the encoding side. For example, a number of analyses have addressed the question whether the distance code follows a linear function or is more complex (e.g. Haldane and Spurway 1954; Frisch and Jander 1957, Schürch et al. 2013; Beekman et al. 2015; Schürch et al. 2019; Kohl and Rutschmann 2021), but in all cases the reference was the physical parameter known by the experimenter (the distance of the feeder for the dancer), not the way in which recruits deal with this information. A more appropriate strategy is obviously to ask the recruits what distance they extract from the message and where they search. Addressing this and other questions of waggle dance communication requires an approach that views decoding as a constructive process, attempting to reveal innate and learned information that controls the recruits' search behavior. Here we approach this question by comparing the two-dimensional density maps (heatmaps) as they result from the encoded vector endpoints with the two-dimensional density maps from both the radar fixes of the endpoints of the vector flights and those of the search flights.

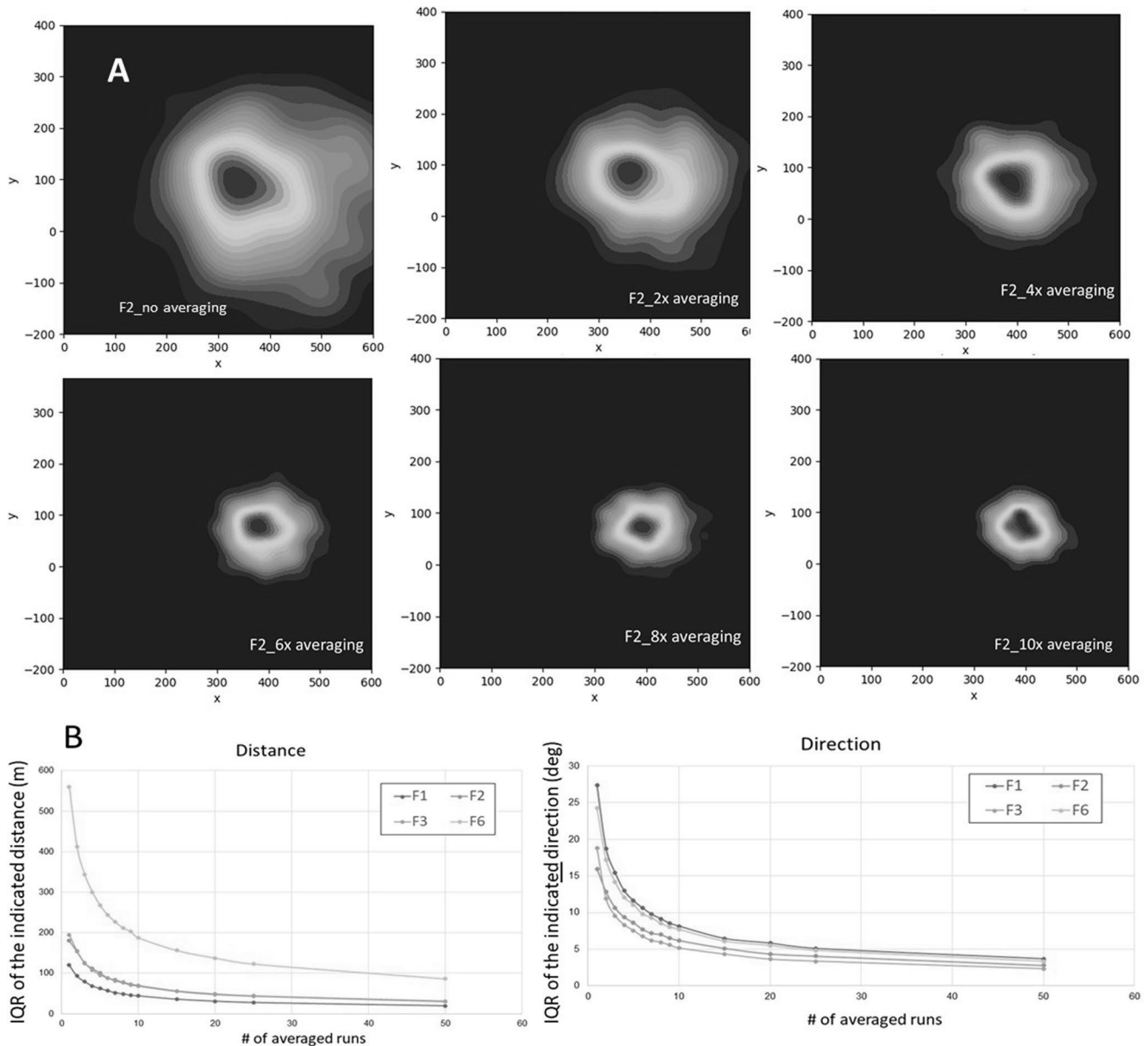


Fig. 8 The effect of the averaging of waggle runs. **A** The effect of averaging as exemplified in heatmaps for F2 recruits. The results for the other feeders are given in Fig. S5. **B** Model calculations of the average-

ing of waggle runs separately for distance and direction for all four feeders. See S7, (for data to Fig. 2 see all tables together to Fig. 2)

Heatmaps of the encoding process have already been used by Schürch et al. (2013; see their Fig. 4). These authors derived the distance function from a Bayesian calibration model using Markov chains that was assumed to converge within the results of a model including 300,000 iterations. The resulting parameter estimates for the distance were found to fit a mixed model that uses a maximum likelihood approach (their Tables 3 and 4). No experimental proof of the model parameters was provided, leaving it open whether the process of decoding by the recruit complied with the assumptions of the model. Similar problems apply to practically all the otherwise highly informative studies of the

encoding process because experimental proof of the decoding processes is lacking (see below).

Our experimental design and the data collected are limited in several senses. It was not possible to record the dance-following of the recruits, whose flight was later reconstructed from harmonic radar tracking. We therefore had limited information about the transmission of the encoded message. However, we can exclude the possibility that the tracked recruits had ever been at the feeding site indicated by the dancing bee other than when flying by during exploration of the environment as a young forager. The number of conditions under which the decoding process was studied is also

rather limited. For example, the distance code may depend on the landscape structure that the foragers experienced during exploratory orientation flights. We examined the effect of the structure of the environment in two ways. (1) The two feeders F1 and F2 were located at roughly similar distances from the hive, but the dancers and recruits flew over very different landscape structures. (2) The feeding sites for the dancers, F1/F2, F3 and F6, were selected such that they were at different distances from the hive and were located differently in relation to salient landmarks. Furthermore, we did not measure the number of dance-followers; the weather conditions were always fine and the motivation to forage was high; the colony conditions differed from a usual bee colony by having 10 times fewer bees and two combs (one on top of the each other) behind a glass window; the dance area of only one side of the comb was observed.

The main results are as follows. (1) Calibrating the dance message by the recruits' search patterns leads to only slightly different results from the approach adopted previously, in which the reference was the geographical location of the feeders indicated by the dancers; the centroid of the search pattern is very close to the feeders' location (Figs. 6, 7 and 8; Fig. S1, S4). (2) The scaling factor converting the number of waggles (as a code of distance) depends on distance, leading to non-linear distance functions (Fig. 4, Fig. S1). (3) The vector flights of the recruits are far from copying the vector information of the dance; they are much shorter particular those towards F1 indicating that vector flight endpoints depend on the landscape structure (Figs. 5 and 6). (4) The deviation of the vector flight from the direct flight to the dance-indicated location is already corrected in the first turn at the beginning of the search flight (Fig. S2). (5) Most importantly, the search flights are much more focused than expected from the two-dimensional distribution of the dance vector endpoints (Fig. 7, Fig. S4). Averaging of the message from several waggle runs is likely the mechanism used by the receivers' search in a more focused way for the dance-indicated location (Fig. 8A, B), but other constructive procedures may be involved. (6) Experience of dance-following one or two days previously is reflected in the search flight density distribution (double peaks of search flight centroids, Fig. 6, Fig. S4). We shall address these results in turn.

Calibrating the distance and direction codes via the centroid of the recruits' search pattern

We calibrated the distance code by defining the distance that is coded by one waggle. The correlation between the number of waggles and the duration of the waggle run is less variable than the duration of the waggle run as usually measured (Menzel and Galizia 2024). Referring to the centroid of the optimal search (closest to the real feeder), we here

introduced the calibrated scaling factor (CSF). Note that all the data in the literature so far are related to the physical distance of and the direction to the dance-indicated feeders, whereas our data relate to the behavior of the recruit. Von Frisch (1967) reports one dataset with the number of waggles as the distance code (p. 100), from which one can read a CSF of 50 m for a distance of 500 m (CSF=63 m), a CSF of 80 m for a distance of 1000 m, and a CSF of 80 m for a distance of 2500 m. Esch (1978) measured close to constant CSFs for five distances (CSF=41 m for 364 m; CSF=41 m for 530; CSF=42 m for 831 m; CSF=43 m for 607 m; CSF=43 for 1077 m). Srinivasan et al. (2000) estimated a CSF slightly increasing with distance (CSF=67 m for 400 m; CSF=70 m for 800 m). Kohl and Rutschmann (2021) determined a constant CSF over distance (according to their Fig. 4a: CSF=44 m for 400 m; CSF=55 m for 800 m; CSF=53 m for 1900 m). We determined a higher CSF for a further distance (F6 2600 m, CSF=80 m) and roughly similar CSF for shorter distances (F1 431 m, CDC: 60 m, F2 387 m CDC=55 m, F3 760 m, CSF=65 m). We draw the following conclusions from the selected CSF values in the literature and our own CSF values: (1) the distance function (distance code vs. geographic or recruits' search centroid) is not a linear function; (2) CSF values based on the physical distance of the feeder tend to be lower than ours based on the recruits' search centroids; (3) overall, the values in the literature are reasonably close to what we found, showing that the dance-followers are surprisingly accurate in their searches.

The angular width of the distribution of the dance vector endpoints decreases with distance. The effect of decreasing the angular spread with distance is small compared to the angular spread that would be necessary to compensate increasing area with distance. The necessary angular spread for F3 would have to be 110° instead of 122°, and for F6 it would have to be 72° instead of 104°, if we take the angular spread to be the same as for F1 and F2 (147° instead of 130°/132°). This result partly supports what has been concluded in the literature (Weidenmüller and Seeley 1999) and speaks against the tuned-error hypothesis as applied to the proposal to adapt the angular error to the distance to keep the search area constant. It thus lends weight to the conclusion drawn by Tanner and Visscher (2010). However, for large distances (e.g. F6: 2600 m) the effect is still considerable. Longer waggle runs may allow more precise reading of the angle relative to gravity, and thus fewer waggle runs to be averaged (Tanner and Visscher 2010). This is what our model calculation of the averaging effect has shown (Figs. 7 and 8A and B). IQRs of longer waggle runs are smaller for direction but not for distance. We may ask why the distance code does not follow this rule. Shorter waggle runs should lead to larger relative variance as compared to longer

waggle runs because the distance code is discrete (number of waggles with CDCs ranging from 60 m to 80 m), which should be reflected in larger variance for shorter distances. In other words, a constant variance of e.g. ± 1 waggle will lead to a relatively lower variance for longer distances. This finding and the role of systematic “errors” may reflect either a distance-dependent effect or cognitive phenomena (see below).

The averaging effect (noise reduction)

A formal way of quantifying the constructive effect in the decoding of the message is to assume that recruits reduce the variance of the message by averaging across several waggle runs, as already suggested by von Frisch and Jander (1957) for the distance and direction code separately. Here we show that evaluating the number of waggle runs followed in one waggle dance leads to a close correspondence with the results of a modeling approach (average number of dance runs followed: 8.5 runs, most gain from averaging: up to 10 runs). Different numbers of rounds followed were observed in other studies: for example, eight rounds by Judd (1994), 17 rounds by Grüter et al. (2008), an average of 2.8 rounds (range 1–16) by Al Toufaily et al. (2013). The most informative data on dance-following come from Biesmeijer and Seeley (2005), who found that the number of dances that were followed and thus potentially averaged depended on the experience of the follower (whether the feeding site was already known to the follower or was novel) and on both the season and the time of the day). Overall, 2–4 dance rounds were followed in their study. These studies are compromised by the same problem that we faced in our study, which is that a dance-follower may have attended more dances before than during the observed dance. In a previous study (Menzel et al. 2011), this problem was solved by training only 2–3 dancers to a novel feeding place and observing all their dances. We found that, after following on average 8.4 rounds (30° experiment) or 16.4 rounds (60° experiment), the followers preferred to fly to the location to which they had been trained before, and after following on average 20.7 rounds (30° experiment) or 23.3 rounds (60° experiment), they always flew toward the dance-indicated location. It thus appears that the large range of dance-following behavior reflects conditions of the communication process that pertain to the evaluation of the information received and the level of experience that the follower has had with the location indicated. The discrepancy between these results and those presented here, as well as the data from earlier studies, argues in favor of additional, unobserved and thus unevaluated dance-following.

Noise reduction during the decoding process could also arise from multisensory integration. The distance is encoded

by multiple parameters (the duration of the waggle rounds, the length and duration of the waggle run, and the number of waggles per run, as evaluated here). Furthermore, different sensory modalities are involved in receiving the waggle run signals, i.e. both mechanical (Esch et al. 1965; Michelsen 2003) and electrostatic signals (Greggers et al. 2013). Averaging and multisensory convergence may reduce uncertainties in the signals, and indeed additional visual signals, a rather artificial condition for *Apis mellifera*, lead to less variance than gravity signals alone (Tanner and Visscher 2010).

Memory of earlier dance-following has also been suggested as a factor in reducing the variance of dances (e.g. Schürch et al. 2013, 2019). Here we document the effect of previous dance-following in the double-peaked distributions of the search flights for F3 and F6 (Figs. 6 and 7, Fig. S4). The dancers for both feeding stations were trained stepwise to the final station, and data were collected after just two days of training to the final location. This was different from the data collection for F1 and F2. Here training lasted at least one week at the final location before the data were collected. F3 was trained in the last step as an extension of the direct line between hive and feeder, and the two density peaks are arranged along this line. In the case of F6, the station before the final station lay to the south of the final station at the same distance along path P3 (see Fig. 1), and the two density peaks are arranged from south to north. Thus, the memory of earlier dance-following must have lasted for at least two days.

Correction of predicted “errors”

The question of whether the variance in the dance message is solely or predominantly determined by the stochastic nature of the encoding process, as apparent to the human observer, has a long tradition in waggle dance analyses (Haldane and Spurway 1954; Frisch and Jander 1957, Tanner and Visscher 2010; De Marco et al. 2008a, Okada et al. 2014; Preece and Beekman 2014) and has been debated intensively. A variation in the dance codes could involve systematic “errors” that may be compensated for by the receiver. For example, the directions of waggle runs depend in a systematic way on (1) their direction in relation to gravity (Markl 1966), (2) the direction of the return run (De Marco et al. 2008b), (3) the motivation of the dancer, as reflected in the speed of dance rounds and controlled by the needs of the colony and the quality of the food (Seeley et al. 2000; Hrncir et al. 2011), (4) the residual misdirection (Lindauer and Martin 1972), and (5) inter-colony differences (Al Toufaily et al. 2013). Therefore, errors as they appear to the human observer may not reflect “noise in the system,” but may carry information. A telling example is the debate about the tuned-error

hypothesis (Haldane and Spurway 1954; Wilson 1962), as applied to the question of whether the dances are for spatially distributed food or localized locations, e.g. a flowering tree, a potential new nest site, distributed flowering plants. The angle of divergence between the directions of the waggle run following a right or left loop of a return run could be a specific indicator of the spatial spread of the indicated goal (Biesmeijer and Seeley 2005).

Potential cognitive effects

A cognitive perspective may be worth considering. Bees leaving the hive explore the environment before they start dance-following and foraging, and thus learn about the sun compass and the landscape features (Capaldi et al. 2000; Degen et al. 2015, 2016). The possibility that recruits had already visited the location of the feeder indicated by the dancer was excluded in our experiments because no natural food sources occurred during the full experimental period within the range of the radar. Recently, it has been found that recruits steer toward the dance-indicated location even when starting from an unexpected release location remote from the hive but within the explored area (Wang et al. 2023). If bees also navigate with the help of a learned map-like memory, the flights of the recruits tested here may also have been guided by a knowledge of the landscape built up during exploratory orientation flights and not only by the dance message. This could mean that the recruits “expect” landscape features at and on the way toward the location indicated by the communicated vector information, a view supported by the different vector flights in the F1 and F2 recruits (Fig. 5, Fig. S2). Thus, this characteristic deviation of the recruits’ search pattern does not reflect a different dance message but is a property of the search. Of course, this result can also be interpreted on an elementary level as the recruits showing an innate tendency to follow elongated ground structures (but see Menzel et al. 2018). Another component of a strategy guiding the recruit could be a shift in search motivation. A hint in this direction comes from the observation that the search pattern changes to some extent in the act of searching, as exemplified by F2 searches (Fig. S3). First, the search becomes more focused, and then it widens again. We did not bait the feeder with food and only a few dancers landed at the feeder. It is tempting to conclude that the problem in finding the dance-indicated feeder leads to a change in search strategy, including a scanning of additional space in accordance with an exploratory motivation.

Embedded in the large datasets documenting a cognitive map in bee navigation (Menzel 2023), this possibility should at least be kept open as a motivation for additional experiments to establish whether recruits retrieve their

landscape memory during dance communication and guide their search pattern accordingly.

Taken together, the averaging of several or many waggle runs within one dance, the operation of convergent stimulus modalities in the receiving animal and the correction of systematic deviations by the receiving animal, the reference to a landscape memory established during exploratory flights, and the occurrence of diverse search strategies may lead to a more precise information transfer and thus to more narrow search areas being covered by the recruits than expected from the variance in the dance message.

Supplementary Information The online version contains supplementary material available at <https://doi.org/10.1007/s00265-025-03593-5>.

Acknowledgements We are grateful for expert assistance during the experiments by Z. Hu and Y. Qu. The honeybee colonies were kindly provided by Dr. R. Büchler, Bieneninstitut Kirchhain, and Landesbetrieb Hessen. We are also grateful to the farmer, Herr Lemmer, who gave us permission to work in his agricultural fields. Thanks go to Dr. Jana Mach and Manu Dür for their help in providing us with useful scripts in Python to analyze the data and prepare the figures. We thank Dr. Rupert Glasgow for helping us with the English.

Author contributions Z.W.: performed experiments, worked on drafts; X.C.: organized data, worked on figures and statistics; R.O.: worked on figures and drafts, performed model calculations; S.W.: ran the harmonic radar; R.M.: designed, supervised and performed the experiments, wrote drafts and final manuscript.

Funding Open Access funding enabled and organized by Projekt DEAL.

ZW was supported by CAS Key laboratory of Tropical Forest Ecology, Xishuangbanna Tropical Garden, CAS “Light of West China” Program (Y6XB081K01) and Yunnan Provincial Science and Technology Department (202105AC160084). XC Scholarship from China Scholarship Council (CSC). RO: financial support from the JSPS KAKENHI (grant number 22K06314). SW: no funding; RM: financial support from the Deutsche Forschungsgemeinschaft Grant Me 49/2 and the Freie Universität Berlin. The authors have no relevant financial or non-financial interests to disclose. The authors have no competing interests to declare that are relevant to the content of this article.

Data availability The data are available in supplement S1.

Declarations

Conflict of interest The authors have no relevant financial or non-financial interests to disclose. The authors have no competing interests to declare that are relevant to the content of this article. All authors certify that they have no affiliations with or involvement in any organization or entity with any financial interest or non-financial interest in the subject matter or materials discussed in this manuscript. The authors have no financial or proprietary interests in any material discussed in this article.

Open Access This article is licensed under a Creative Commons Attribution 4.0 International License, which permits use, sharing, adaptation, distribution and reproduction in any medium or format, as long as you give appropriate credit to the original author(s) and the

source, provide a link to the Creative Commons licence, and indicate if changes were made. The images or other third party material in this article are included in the article's Creative Commons licence, unless indicated otherwise in a credit line to the material. If material is not included in the article's Creative Commons licence and your intended use is not permitted by statutory regulation or exceeds the permitted use, you will need to obtain permission directly from the copyright holder. To view a copy of this licence, visit <http://creativecommons.org/licenses/by/4.0/>.

References

- Al Toufaily H, Couvillon MJ, Ratnieks FL, Grüter C (2013) Honey bee waggle dance communication: signal meaning and signal noise affect dance follower behaviour. *Behav Ecol Sociobiol* 67:549–556
- Beekman M, Makinson JC, Couvillon MJ, Preece K, Schaerf TM (2015) Honeybee linguistics—a comparative analysis of the waggle dance among species of *Apis*. *Front Ecol Evol* 3:11
- Biesmeijer JC, Seeley TD (2005) The use of waggle dance information by honey bees throughout their foraging careers. *Behav Ecol Sociobiol* 59:133–142
- Capaldi EA, Smith AD, Osborne JL, Fahrbach SE, Farris SM, Reynolds DR, Edwards AS, Martin A, Robinson GE, Poppy GM, Riley JR (2000) Ontogeny of orientation flight in the honeybee revealed by harmonic radar. *Nature* 403:537–540
- Chatterjee A, George EA, MV P, Basu P, Brockmann A (2019) Honey bees flexibly use two navigational memories when updating dance distance information. *J Exp Biol* 222:jeb195099
- Cheeseman JF, Winnebeck EC, Millar CD, Kirkland LS, Sleigh J, Goodwin M, Pawley MD, Bloch G, Lehmann K, Menzel R, Warman GR (2012) General anesthesia alters time perception by phase shifting the circadian clock. *Proceedings of the National Academy of Sciences USA* 109:7061–7066
- Couvillon MJ, Riddell Pearce FC, Harris-Jones EL, Kuepfer AM, Kenzie-Smith SJ, Rozario LA, Schürch R, Ratnieks FL (2012) Intra-dance variation among waggle runs and the design of efficient protocols for honey bee dance decoding. *Biology Open* 1:467–472
- De Marco RJ, Gurevitz JM, Menzel R (2008) Variability in the encoding of spatial information by dancing bees. *J Exp Biol* 211:1635–1644
- Degen J, Kirbach A, Reiter L, Lehmann K, Norton P, Storms M, Koblofsky M, Winter S, Georgieva PB, Nguyen H, Chamkhi H, Greggers U, Menzel R (2015) Exploratory behaviour of honeybees during orientation flights. *Anim Behav* 102:45–57
- Degen J, Kirbach A, Reiter L, Lehmann K, Norton P, Storms M, Koblofsky M, Winter S, Georgieva PB, Nguyen H, Menzel R (2016) Honeybees learn landscape features during exploratory orientation flights. *Curr Biol* 26:2800–2804
- Esch H (1978) On the accuracy of the distance message in the dances of honey bees. *J Comp Physiol A* 123:339–347
- Esch H, Esch I, Kerr WE (1965) Sound: an element common to communication of stingless bees and to dances of the honey bee. *Science* 149:320–321
- Frisch K, Jander R (1957) über Den Schwänzeltanz der Bienen. *Z Für Vergleichende Physiologie* 40:239–263
- Greggers U, Koch G, Schmidt V, Durr A, Floriou-Servou A, Piepenbrock D, Gopfert MC, Menzel R (2013) Reception and learning of electric fields in bees. *Proceedings of Royal Society Biological Science* 280:20130528
- Grüter C, Balbuena MS, Farina WM (2008) Informational conflicts created by the waggle dance. *Proc Royal Soc Biol Sci* 275:1321–1327
- Haldane JB, Spurway H (1954) A statistical analysis of communication in *Apis mellifera* and a comparison with communication in other animals. *Insectes Sociaux* 1:247–283
- Hrncir M, Maia-Silva C, McCabe SI, Farina WM (2011) The Recruiter's excitement—features of thoracic vibrations during the honey Bee's waggle dance related to food source profitability. *J Exp Biol* 214:4055–4064
- Judd TM (1994) The waggle dance of the honey bee: which bees following a dancer successfully acquire the information? *J Insect Behav* 8:343–354
- Kohl PL, Rutschmann B (2021) Honey bees communicate distance via non-linear waggle duration functions. *PeerJ* 9:e11187
- Lindauer M, Martin H (1972) Magnetic effect on dancing bees. NASA, Washington Animal Orientation and Navigation
- Markl H (1966) Schwerkraftdressuren an Honigbienen i.die geomotaktische fehlorientierung. *Z Vergl Physiol* 53:328–352
- Menzel R (2023) Navigation and dance communication in honeybees: a cognitive perspective. *J Comp Physiol A* 209:1–13
- Menzel R, Galizia CG (2024) Landmark knowledge overrides optic flow in honeybee waggle dance distance Estimation. *J Exp Biol* 227(21):jeb248162
- Menzel R, Kirbach A, Haass W-D, Fischer B, Fuchs J, Koblofsky M, Lehmann K, Reiter L, Meyer H, Nguyen H, Jones S, Norton P, Greggers U (2011) A common frame of reference for learned and communicated vectors in honeybee navigation. *Curr Biol* 21:645–650
- Menzel R, Tison L, Fischer-Nakai J, Cheeseman J, Lehmann K, Balbuena MS, Chen X, Landgraf T, Petrasch J, Greggers U (2018) Honeybees are guided by learned elongated ground structures. *Front Behav Neurosci* 12:322–336
- Michelsen A (2003) Signals and flexibility in the dance communication of honeybees. *J Comp Physiol A* 189:165–174
- Okada R, Ikeno H, Kimura T, Ohashi M, Aonuma H, Ito E (2014) Error in the honeybee waggle dance improves foraging flexibility. *Sci Rep* 4:4175
- Preece K, Beekman M (2014) Honeybee waggle dance error: adaption or constraint? Unravelling the complex dance Language of honeybees. *Anim Behav* 94:19–26
- Riley JR, Greggers U, Smith AD, Stach S, Reynolds DR, Stollhoff N, Brandt R, Schaupp F, Menzel R (2003) The automatic pilot of honeybees. *Proc Royal Soc Biol Sci* 270:2421–2424
- Riley JR, Greggers U, Smith AD, Reynolds DR, Menzel R (2005) The flight paths of honeybees recruited by the waggle dance. *Nature* 435:205–207
- Schürch R, Couvillon MJ, Burns DD, Tasman K, Waxman D, Ratnieks FL (2013) Incorporating variability in honey bee waggle dance decoding improves the mapping of communicated resource locations. *J Comp Physiol A* 199:1143–1152
- Schürch R, Ratnieks FL, Samuelson EE, Couvillon MJ (2016) Dancing to her own beat: honey bee foragers communicate via individually calibrated waggle dances. *J Exp Biol* 219:1287–1289
- Schürch R, Zwirner K, Yambrick BJ, Pirault T, Wilson JM, Couvillon MJ (2019) Dismantling babel: creation of a universal calibration for honey bee waggle dance decoding. *Anim Behav* 150:139–145
- Seeley TD, Mikheyev AS, Pagano GJ (2000) Dancing bees tune both duration and rate of waggle-run production in relation to nectar-source profitability. *J Comp Physiol A* 186:813–819
- Srinivasan MV, Zhang S, Altwein M, Tautz J (2000) Honeybee navigation: nature and calibration of the odometer. *Science* 287:851–853
- Strecha C, Küng O, Fua P (2012) Automatic mapping from ultra-light UAV imagery. In
- Su P-F, Lin C-CK, Hung J-Y, Lee J-S (2022) The proper use and reporting of survival analysis and Cox regression. *World Neurosurg* 161:303–309

- Tanner DA, Visscher PK (2008) Do honey bees average directions in the waggle dance to determine a flight direction? *Behav Ecol Sociobiol* 62:1891–1898
- Tanner DA, Visscher PK (2010) Adaptation or constraint? Reference-dependent scatter in honey bee dances. *Behav Ecol Sociobiol* 64:1081–1086
- von Frisch K (1923) Über die sprache der Bienen - Eine tierpsychologische untersuchung. *Zool Jb* 40:1–186
- von Frisch K (1967) The dance Language and orientation of bees. Harvard Univ., Cambridge
- Wang Z, Chen X, Becker F, Greggers U, Walter S, Werner M, Gallistel CR, Menzel R (2023) Honey bees infer source location from the dances of returning foragers. *Proc Natl Acad Sci USA* 120(12):1–8. e2213068120
- Weidenmuller A, Seeley TD (1999) Imprecision in waggle dances of the honeybee (*Apis mellifera*) for nearby food sources: error or adaptation? *Behav Ecol Sociobiol* 46:190–199
- Wilson EO (1962) Chemical communication among workers of the fire ant *Solenopsis saevissima* (Fr. Smith) 2. An information analysis of the odour trail. *Anim Behav* 10:148–158

Publisher's note Springer Nature remains neutral with regard to jurisdictional claims in published maps and institutional affiliations.